

LASER FOOTPRINT SIZE AND POINTING PRECISION ANALYSIS FOR LIDAR SYSTEMS

Xu Bin ^a, Li Fangfei ^a, Zhang Keshu ^{a*}, Lin Zongjian ^b

^a Academy of Opto-electronics, Chinese Academy of Sciences, 95, Zhongguancun Road East, Haidian District, Beijing, China, 100080 - xub@aoe.ac.cn

^b Chinese Academy of Surveying & Mapping, 16 Beitaping Road, Beijing, China, 100039 - lincasm@casm.ac.cn

WG I/2 - SAR and LiDAR Systems

KEY WORDS: LiDAR, Data, Accuracy, Analysis, Laser scanning

ABSTRACT:

Laser footprint size and beam divergence angle tuning was found to affect LiDAR data accuracy and measurement precision because of beam axis shifting. The laser beam divergence angle is generally tunable in modern LiDAR systems in order to adapt to different application scenarios. Beam divergence angle can either be switched from one position to the other (i.e. 0.3mRad / 0.8 mRad), or be tuned continuously (i.e. 0.3 to 0.8 mRad). In either case, mechanical moving parts have to be introduced into the optical systems. As a result, the movements of mechanical parts make the optical axis shift and the laser pointing direction shift as well. In other words, switching laser beam divergence angle makes the laser pointing accuracy degrade. A mathematic model was developed to improve the LiDAR data accuracy when the laser beam divergence angle was changed in surveying practice. Experiments were designed and carried on to verify the calibration model. A calibration method and procedure was introduced to handle these issues.

1. INTRODUCTION

In the last few years, some of the weaknesses of photogrammetry have been overcome by using airborne LiDAR (Light Detection And Ranging) (Baltsavias, 1999a), which proves that laser altimetry is now a mature technology for the determination of accurate DTMs. The term airborne LiDAR or Airborne Laser Scanning (ALS) refers to an airborne laser system consisting of a laser scanner, a geodetic-quality GPS receiver and an inertial measurement unit (IMU), which provide data about the scan angle and the aircraft coordinates and attitude (Wehr and Lohr, 1999). Based on this data and on the distances measured, point coordinates are calculated (Baltsavias, 1999b) and stored in digital format in the onboard computer.

LiDAR systems are widely used in modern surveying projects due to its accuracy, informative signals and good resolution. People are interested in acquiring higher accuracy in measuring, pointing, more return signals and better resolution of intensity. Laser footprint size and beam divergence angle tuning was found to affect LiDAR data accuracy and measurement precision through its influence on laser beam pointing.

Besides the consideration of human-eye safety, laser power, flying altitude, point cloud distribution etc., the geometric feature of survey targets is the primary factors determining the LiDAR's beam divergence angle. For city survey projects, it is desirable to get accurate 3-D models of the buildings, streets, rivers and so on. The edges of models should be as sharp as possible when they are extracted from the LiDAR shots cloud. Small footprint size and high shot cloud density are the precondition for this purpose. In the forest survey, laser beam should have a small divergence angle to get the hierarchy, multi-return signals and high penetrability. In electric wire survey, bigger footprint should be used to detect the small targets.

The laser beam divergence angle is generally tunable in modern LiDAR systems in order to adapt to above application scenarios. Beam divergence angle can either be switched from one position to the other (i.e. 0.3mRad / 0.8 mRad), or be tuned continuously (i.e. 0.3 to 0.8 mRad). In either case, mechanical moving parts have to be introduced into the optical systems. As a result, the movement of mechanical parts made the optical axis shift and the laser pointing direction shift at the same time. In other words, switching laser beam divergence angle made the laser pointing accuracy degraded. Taking AOE-LiDAR system as an example, 0.1 mm offset at the emission point (about 0.218mRad offset) of laser beam expander caused 0.28m of error in 1000 meters distance and 0.56m in 2000 meters away. Moreover, the offset did not occur just along the x or z axis, it occurred in any direction.

There are several error sources that can degrade the accuracy of the derived ground coordinates (Nora Csanyi May, Charles K. Toth, 2007), such as, errors in the navigation solution (position and attitude errors), range measurement errors, scale and offset errors of scan angle, etc. In addition, the effect of the errors is influenced by the flight parameters (flying height, flying speed, etc.). Usually, the basic errors such as range measurement errors, scale and offset errors of scan angle were calibrated in lab calibration, the navigation errors were calibrated in flight. Because of the complex error sources, it is hard to separate the error brought by the change of beam divergence in flight calibration; and because of the limited space in lab, this error can not be calibrated in lab either. A better method to calibrate the laser pointing error was a calibration experiment on field.

2. METHODOLOGY

As shown in Figure 1, the optical system of typical LiDAR system includes a laser transmitter, a set of lenses, a fixed

mirror and a swinging mirror. When tuning beam divergence, actually the lenses in the beam expander were moving.

To calculate the effect of the errors caused by the change of divergence angle, a scan coordinate system was established first. Taking the incidence point on the fixed mirror as the origin point, defined the direction of flight as X axis while Y axis pointed to the larboard, and Z axis pointed to the opposite direction of the transmitted laser beam.

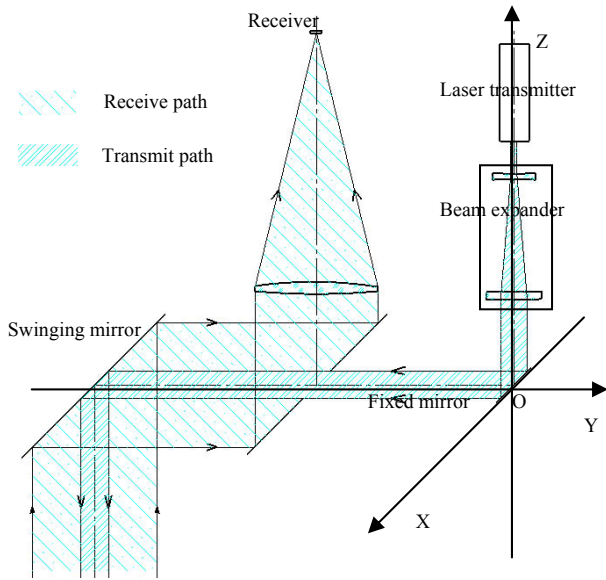


Figure 1. The mechanical system of AOE-LiDAR, including a laser transmitter, a set of lenses, a fixed mirror and a swinging mirror.

The scan coordinate system is shown in Figure 2, M1 represented the fixed mirror; M2 represented the swinging mirror. To simplify the geometry model of the mechanical system, only the errors of the direction of the laser beam were considered. These errors caused the incidence point depart from the origin, which was its initial position; these departures composed the error vector $E = [e_1 \ e_2]$. E was on the plane of M1, with the positive direction of e_1 was along the X axis, the positive direction of e_2 was along the projection of Y axis on the M1 plane.

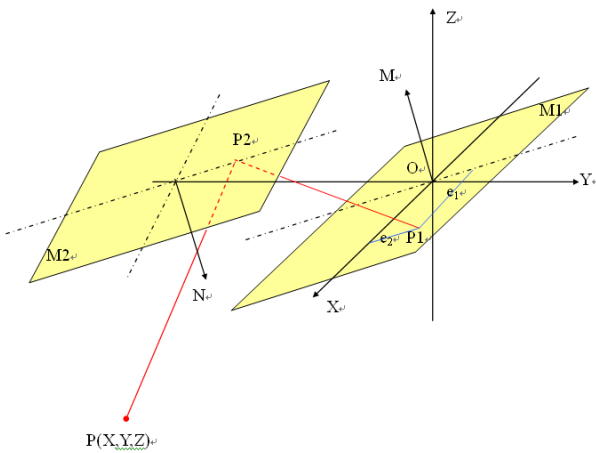


Figure 2. The scan coordinate system of the mechanic structure

The fixed mirror M1 with normal vector $M = [m_1 \ m_2 \ m_3]$ was described by

$$m_1x + m_2y + m_3z = 0 \quad (1)$$

The beginning point of the distance measurement was defined as $O = [X_o \ Y_o \ Z_o]$; the true incidence direction vector ($\vec{i} = [i_1 \ i_2 \ i_3]$) was represented by a function of O and E,

$$\vec{i} = f(O, E) \quad (2)$$

The incidence point ($P_1 = [X_1 \ Y_1 \ Z_1]$) on M1 was a function of E,

$$P_1 = g(E) \quad (3)$$

With M1 considered as a plane, the direction of the reflected laser beam $\vec{o} = [o_1 \ o_2 \ o_3]$ was given by \vec{i} and M.

This laser beam then arrived at the swinging mirror M2, and was reflected again. M2 swung at a certain angular velocity around the X axis. The position of M2 was given by the beginning normal vector N_0 and the swing angle ω , so the current normal vector of M2 was $N = [n_1 \ n_2 \ n_3] = R_\omega \cdot N_0$ where R_ω was the swing angle matrix, and the function of M2 was

$$n_1(x - X_1) + n_2(y - Y_1) + n_3(z - Z_1) = 0 \quad (4)$$

The incident laser beam of M2 was given by P_1 and \vec{o} , the position of the incidence point on M2 was $P_2 = [X_2 \ Y_2 \ Z_2]$. The direction of the reflected laser beam was $\vec{s} = [s_1 \ s_2 \ s_3]$.

Defining P as the target point coordinate with $[X_p \ Y_p \ Z_p]$, and the distance between P_2 and P was d, then

$$P = P_2 + \vec{s} \cdot d \quad (5)$$

All the calculations above were processed in the scan coordinate system, while the measurement was done in another coordinate system called the ground system (which was a local coordinate system defined by total station), so the coordinate of P had to be translated into this system. The target point in the ground coordinate system was defined by function

$$\bar{P} = R_{\omega_x} R_{\phi_y} R_{\kappa_z} \cdot P + D \quad (6)$$

Where $\omega_g, \varphi_g, \kappa_g$ were the angles between XYZ axes of the two coordinate systems, and $R_{\omega_g}, R_{\varphi_g}, R_{\kappa_g}$ were the circumrotate matrices; $D = [X_0 \ Y_0 \ Z_0]$ was the displacement vector.

The coordinate of target point P with the errors E was given by function (6), the simplified form was,

$$\bar{P} = G(e_1, e_2) \tag{7}$$

$$G = G_0 + \frac{\partial G}{\partial e_1} \Delta e_1 + \frac{\partial G}{\partial e_2} \Delta e_2$$

where

Define an error correction vector as

$$V = AX - L \tag{8}$$

where

$$A = \begin{bmatrix} \frac{\partial G_x}{\partial e_1} & \frac{\partial G_x}{\partial e_2} \\ \frac{\partial G_y}{\partial e_1} & \frac{\partial G_y}{\partial e_2} \\ \frac{\partial G_z}{\partial e_1} & \frac{\partial G_z}{\partial e_2} \end{bmatrix}$$

$$X = [\Delta e_1 \ \Delta e_2]^T$$

$$L = \begin{bmatrix} l_x \\ l_y \\ l_z \end{bmatrix} = \begin{bmatrix} G_x - (G_x) \\ G_y - (G_y) \\ G_z - (G_z) \end{bmatrix} = \begin{bmatrix} \bar{X} \\ \bar{Y} \\ \bar{Z} \end{bmatrix} - R_g \begin{bmatrix} X_p \\ Y_p \\ Z_p \end{bmatrix} - \begin{bmatrix} X_0 \\ Y_0 \\ Z_0 \end{bmatrix}$$

$$R_g = R_{\varphi_g} R_{\omega_g} R_{\kappa_g} = \begin{bmatrix} \cos \varphi_g & 0 & -\sin \varphi_g \\ 0 & 1 & 0 \\ \sin \varphi_g & 0 & \cos \varphi_g \end{bmatrix} \begin{bmatrix} 1 & 0 & 0 \\ 0 & \cos \omega_g & -\sin \omega_g \\ 0 & \sin \omega_g & \cos \omega_g \end{bmatrix} \begin{bmatrix} \cos \kappa_g & -\sin \kappa_g & 0 \\ \sin \kappa_g & \cos \kappa_g & 0 \\ 0 & 0 & 1 \end{bmatrix}$$

To calculate the errors, firstly gave original values of them by experience, then got the increment,

$$X = (A^T A)^{-1} A^T L \tag{9}$$

Use X to correct the original values of the errors, then iterate the calculation until the error reaches the expected accuracy.

3. EXPERIMENT

3.1 The LiDAR

The AOE-LiDAR, which was developed by Academy of Opto-Electronics, Chinese Academy of Sciences, consists of three main data source (sensors). The first one is a laser scanner that provides range information from the laser beam firing point to the object point. The second one is a GPS that relates the range information to the ground reference frame, and thirdly, an IMU

unit supplies the total system with attitude information. The feature of the AOE-LiDAR used in the experiment is described in the datasheet below.

Weight	Control Pack: 60kg Sensor Pack: 25.5kg
Dimensions L × W × H (mm)	Sensor pack: 316 × 290 × 480 Control pack: 600 × 610 × 615
Power requirements	28VDC, 30A(maximum)
Wavelength	1064 nm
Laser repetition rate	33kHz (max, altitude 3.5km) 50kHz (max, altitude 2.5km) 70kHz (max, altitude 1.7km) 100kHz (max, altitude 1.1km)
Beam divergence	Dual divergence 0.3mrad or 0.8mrad
Operation altitude	200~3,000m nominal
Scan angle	Variable, from 0 to ±25°

Table 1. Datasheet of the AOE-LiDAR

3.2 Experiment method

The experiment was operated on field to ensure the distance between the LiDAR and the target wall was at least 200 meters (the minimum measurement range of AOE-LiDAR), as shown in Figure 3. The LiDAR sensor was placed on a tripod with the -Z axis towards front, the +X axis towards up. When started scanning, the beam went horizontally and the footprints on the wall composed a nearly horizontal line.



Figure 3. AOE-LiDAR in the experiment field

The target points on the wall were marked by retro-reflectors, as shown in Figure 4. And a total station was used to measure the footprint on the wall accurately.

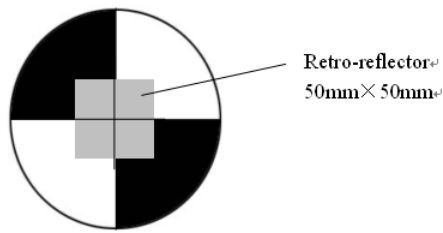


Figure 4. The retro-reflector placed on the wall

In the experiment, there are two steps continuously collecting data. In the first step, the beam divergence angle was set to 0.3mrad; the incidence point on M1 was defined as the origin in Figure.1. Set the scan angle to a fixed value, the coordinate of the point could be calculated from the recorded angle and range of the target.

In the second step the beam divergence angle was set to 0.8mrad; set the scan angle to the same value as before. For the errors caused by movement of the incidence point on M1, the true coordinate of the point was changed. The footprint movement direction on the wall was observed by infrared observer. This helped to make sure that the tuning of beam divergence affected the laser pointing accuracy.

3.3 The Experiment Data

In the experiment, 31 points were set from -15° to 15° with a gain of 1° . Two groups of data were recorded in order to calculate the error vector E.

One group was the target point coordinates recorded by AOE-LiDAR (with errors caused by the change of beam divergence angle). The scan angle and range recorded by AOE-LiDAR are shown in Table.2.

No.	1	2	3	4	5
Angle (°)	-7.5	-7	-6.5	-6	-5.5
Range(mm)	222235	221296	220425	219631	218906
6	7	8	9	10	11
-5	-4.5	-4	-3.5	-3	-2.5
218269	217679	217175	216731	216358	216058
12	13	14	15	16	17
-2	-1.5	-1	-0.5	0	0.5
215811	215632	215532	215489	215505	215601
18	19	20	21	22	23
1	1.5	2	2.5	3	3.5
215739	215966	216254	216604	217026	217517
24	25	26	27	28	29
4	4.5	5	5.5	6	6.5
218071	218712	219396	220168	221010	221934
30	31				
7	7.5				
222925	223990				

Table 2. Scan angle and range recorded by AOE-LiDAR

If the errors caused by the change of beam divergence angle were not considered, the point coordinates were calculated as shown in Table 3.

No.	1	2	3	4	5
X(mm)	1679.7	1676.7	1673.7	1670.7	1667.8
Y(mm)	-37947.6	-33965	-30014.3	-26093.3	-22199.3
Z(mm)	-213984.4	-213914.5	-213842.3	-213771.3	-213700
6	7	8	9	10	11
1664.9	1661.9	1659.1	1656.2	1653.3	1650.5
-18331.4	-14482.5	-10655.1	-6843.2	-3046.1	738.9
-213641.7	-213564	-213505.3	-213436.4	-213372.3	-213312.2
12	13	14	15	16	17
1647.6	1644.8	1641.9	1639.1	1636.3	1633.4
4515	8283.6	12047.1	15808.1	19568.5	23331.4
-213240.3	-213170	-213113.1	-213047.5	-212976.7	-212918.7
18	19	20	21	22	23
1630.6	1627.7	1624.9	1622	1619.1	1616.3
27097.2	30870.8	34653.1	38446	42252.8	46076
-212837.2	-212778	-212713.6	-212643.8	-212577.7	-212513.2
24	25	26	27	28	29
1613.4	1610.4	1607.5	1604.6	1601.6	1598.6
49916.5	53781.2	57664.4	61576.9	65516.9	69490.6
-212442.1	-212387.7	-212307.4	-212242.9	-212172	-212109.6
30	31				
1595.6	1592.5				
73496.6	77538.8				
-212038.1	-211963.1				

Table 3. Point coordinates calculated without considering errors caused by e_1 and e_2

The other group was the coordinates measured by total station. The true coordinates of the target point measured by total station were shown in Table.4.

No.	1	2	3	4	5
X(mm)	1700	1697	1696	1694	1690
Y(mm)	-37913	-33929	-29977	-26058	-22164
Z(mm)	-213987	-213921	-213848	-213780	-213709
6	7	8	9	10	11
1687	1682	1679	1677	1677	1670
-18296	-14449	-10620	-6809	-3010	773
-213652	-213568	-213507	-213440	-213373	-213316
12	13	14	15	16	17
1667	1667	1666	1661	1658	1657
4550	8319	12083	15844	19602	23367
-213242	-213171	-213111	-213044	-212973	-212915
18	19	20	21	22	23
1650	1648	1645	1643	1641	1637
27134	30907	34690	38481	42288	46112
-212834	-212775	-212706	-212641	-212574	-212506
24	25	26	27	28	29
1633	1632	1629	1626	1624	1620
49952	53818	57700	61612	65554	69525
-212438	-212384	-212301	-212231	-212163	-212101
30	31				
1619	1617				
73532	77576				
-212030	-211952				

Table 4. Point coordinates measured by total station

Use these two groups of data, the errors were calculated by the formulae (1) ~ (9).

3.4 Results

From Table.3 and Table.4, the errors e_1 and e_2 described in chapter 2 were calculated. Since the values of the errors were usually small judged by experience, the initial values of e_1 and e_2 were set to zero. After several times of iteration, e_1 and e_2 were calculated as $e_1 = 0.036793040994718$ (mm), $e_2 = 0.066471918809104$ (mm). Recalculate the scan point

coordinates by adding the effect e_1 and e_2 , the calibrated point coordinates were shown in Table 5.

No.	1	2	3	4	5
X(mm)	1701.6	1698.5	1695.4	1692.4	1689.4
Y(mm)	-37911.6	-33929.9	-29978.3	-26057.9	-22163.6
Z(mm)	-213991.2	-213924.7	-213847.9	-213778.5	-213705.5
6	7	8	9	10	11
1686.4	1683.4	1680.5	1677.6	1674.7	1671.8
-18295.9	-14446.9	-10619.4	-6807.7	-3010.4	774.5
-213647.4	-213568.6	-213507.9	-213439.8	-213372.2	-213314.4
12	13	14	15	16	17
1668.9	1666	1663.2	1660.3	1657.5	1654.7
4550.6	8319.2	12082.6	15843.6	19604	23366.9
-213241.7	-213171.4	-213113.6	-213047.8	-212975.2	-212917.1
18	19	20	21	22	23
1651.8	1649	1646.2	1643.4	1640.5	1637.7
27132.7	30906.3	34688.3	38481.5	42288.4	46111.2
-212834.9	-212775.2	-212707.9	-212640.1	-212574.1	-212506.4
24	25	26	27	28	29
1634.9	1632	1629.1	1626.3	1623.4	1620.5
49952	53816.7	57699.9	61611.9	65552.7	69525.8
-212436.1	-212381.4	-212300.6	-212232.9	-212165.3	-212099.4
30	31				
1617.5	1614.6				
73532	77573.8				
-212028.4	-211951.4				

Table 5. Point coordinates calibrated by e_1 and e_2

In Figure.5, the true values (point coordinates measured by total station) were represented by data set 1; the raw data (point coordinates calculated without considering e_1 and e_2) were represented by data set 2; the calibrated data (point coordinates calculated considering e_1 and e_2) were represented by data set 3.

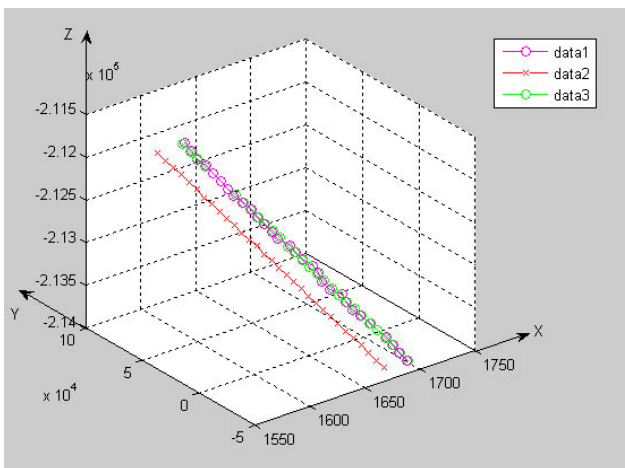


Figure 5 . The errors caused by change of beam divergence angle before and after calibration

4. DISCUSSION

From the data above, obvious system errors were found when tuning the beam divergence of LiDAR; actually the errors were caused by the shift of the optical axis. It was hard to make the incidence point on the mirror immobile when tuning beam divergence. From the experiment, shift of the incidence point was calculated, error vector E was added to formula (6), the errors of recalculated scan points were reduced. The pointing

accuracy of AOE-LiDAR is required to be 0.1mRad; that means at the distance of 200m, the errors on X axis and Y axis were less than 20mm. Before calibration, the residuals were $dx = \pm 21.5\text{mm}$, $dy = \pm 35.5\text{mm}$, $dz = \pm 5.2\text{mm}$. After calibration, the residuals reduced to $dx = \pm 1.2\text{mm}$, $dy = \pm 0.8\text{mm}$, $dz = \pm 1.6\text{mm}$. That satisfied the pointing accuracy of AOE-LiDAR.

In future research, an improved calibration method will be studied, which contained the error factors in a general mathematic model. The relativity between the error factors is complex; the general mathematic model would help to increase the LiDAR data precision.

5. CONCLUSIONS

When tuning the beam divergence angle (which changed the footprint size), the movement of mechanical parts made the optical axis shift and the laser pointing direction shift at the same time. In other words, switching laser beam divergence angle made the laser pointing accuracy degraded. From formulae (1) ~ (9), the optical axis shifting errors were calculated in the ground experiment. After calibration the system error caused by vector E was removed, the pointing precision of AOE-LiDAR increased obviously, which was increased from $\pm 0.2\text{mRad}$ to $\pm 0.01\text{mRad}$.

REFERENCES

Baltsavias, E.P., 1999a. A comparison between photogrammetry and laser scanning. *ISPRS Journal of Photogrammetry and Remote Sensing*, 54, 83-94.

Baltsavias, E.P., 1999b. Airborne laser scanning: basic relations and formulas. *ISPRS Journal of Photogrammetry and Remote Sensing*, 54, 199-214.

Burman, H., 2000. Calibration and Orientation of Airborne Image and Laser Scanner Data Using GPS and INS, *PhD dissertation, Photogrammetry Reports No. 69, Royal Institute of Technology, Stockholm*, 107p.

Luis Gonçalves-Seco, David Miranda, Rafael Crecente and Javier Farto. Digital Terrain Model generation using airborne LiDAR in a forested area of Galicia, Spain. *7th International Symposium on Spatial Accuracy Assessment in Natural Resource and Environmental Sciences*, 169-180.

Nora Csanyi May, Charles K. Toth, 2007. Point Position Accuracy of Airborne LiDAR Systems: A Rigorous Analysis. *International Archives of Photogrammetry, Remote Sensing and Spatial Information Sciences*, 36, 107-111.

Wehr, A., Lohr, U., 1999. Airborne laser scanning - an introduction and overview. *ISPRS Journal of Photogrammetry and Remote Sensing*, 54, 68-82.

ACKNOWLEDGEMENTS

The authors would like to thank the LiDAR Department, Academy of Opto-Electronics, Chinese Academy of Sciences for having supported LiDAR data acquisition.

